Alternative method to calculate the magnetic field of permanent magnets with azimuthal symmetry

J. M. Camacho and V. Sosa[a]
Facultad de Ingeniería, Universidad Autónoma de Yucatán,
Av. Industrias no contaminantes por Periférico Norte, A.P. 150 Cordemex, Mérida, Yuc., México.
[a]*Permanent address: Departamento de Física Aplicada, CINVESTAV-IPN,*
Unidad Mérida, A.P. 73 Cordemex, Mérida, Yuc., C.P. 97310, México.
Phone: (+52-999) 9429445; Fax: (+52-999) 9812917.
e-mail: vic@mda.cinvestav.mx.

Received 6 September 2012; accepted 8 January 2013

The magnetic field of a permanent magnet is calculated analytically for different geometries. The cases of a sphere, cone, cylinder, ring and rectangular prism are studied. The calculation on the axis of symmetry is presented in every case. For magnets with cylindrical symmetry, we propose an approach based on an expansion in Legendre polynomials to obtain the field at points off the axis. The case of a cylinder magnet was analyzed with this method by calculating the force between two magnets of this shape. Experimental results are presented too, showing a nice agreement with theory.

Keywords: Permanent magnet; calculation; analytical; symmetry.

PACS: 75.50 Ww; 41.20 Gz.

1. Introduction

Since ancient times, magnetism has captured the interest of human beings. The feeling of an unseen force (but no less invisible than the force of gravity) acting with great intensity, is often astonishing. The properties of magnetite, an iron mineral used as the needle in a compass, were known since the eleventh century A. D. Over years, knowledge of magnetic phenomena has opened new perspectives and has encouraged the development of new technologies. For example we now know that some living organisms have small amounts of magnetite in their tissues and use it to orient in the Earth's magnetic field. Bees, salmons and some turtles are a few examples of such species [1]. The effect of magnetic fields on water is a topic of current research too [2-4]. For example, it has been found that these fields inhibit scale formation, by inducing changes in the crystal structure of carbonate in the liquid. On the other hand, other researchers investigate to what extent cell phones and magnetism from electric power lines affect living things. The development of technology has brought many important magnetic applications like electric motors, generators and storage of information. However, it is not easy to find in the literature information about the magnetic fields produced by these magnets. Generally, these fields are calculated by numerical methods, such as the finite-element method, [5,6] and it is rare to find analytical expressions. The most known cases are the spherical and the rectangular prism magnets. The field of a ring-shaped magnet has been discussed recently [7,8]. This paper is focused on the analytical calculation of the field produced by permanent magnets with different shapes. We studied $Nd_2Fe_{14}B$ permanent magnets with the following geometries: sphere, cylinder, ring, cone and rectangular prism. The aim was to develop an alternative method of calculation and find analytical expressions for these fields. This will allow estimation of many important variables in certain applications, such as the force between magnets. We will see that the results obtained theoretically and experimentally are consistent with each other.

2. Theory

Typically, the magnetic field of a permanent magnet can be calculated from the vector potential: $\vec{B} = \nabla \times \vec{A}$. For a body whose magnetization is constant inside its volume and drops abruptly to zero outside it, as is the case of a magnet, this potential at point $\vec{x}$ is given by the following surface integral [9]:

$$\vec{A}(\vec{x}) = \frac{\mu_0}{4\pi} \oint \frac{\vec{M}(\vec{x'}) \times \hat{n'}}{|\vec{x} - \vec{x'}|} da'$$

where $\vec{M}$ is the volume magnetization of the magnet, $\hat{n'}$ is the unit vector normal to the surface at point $\vec{x'}$, and μ_0 is the vacuum magnetic susceptibility. The integral is performed over the entire surface of the magnet. In this work we adopt a different method. It is assumed that the magnet is a continuous distribution of dipoles, which occupy a volume dV and have a magnetic dipole moment $d\vec{m} = \vec{M} dV$. Again, here we assume that the magnetization is constant, and it remains unchanged for any external magnetic field. That is, the magnets are supposed to be hard. To facilitate the calculations, we always choose $\vec{M} = M\hat{k}$. As a starting point, we recall that the magnetic scalar potential and the induction field at point $\vec{x}$ produced by a magnetic dipole located at the origin are given by:

$$\Phi_{\text{dipole}}(\vec{x}) = \frac{1}{4\pi}\frac{\vec{m}\cdot\hat{n}}{|\vec{x}|^2},$$
$$\vec{B}_{\text{dipole}}(\vec{x}) = \frac{\mu_0}{4\pi}\frac{3\hat{n}(\hat{n}\cdot\vec{m})-\vec{m}}{|\vec{x}|^3} \quad (1)$$

where $\vec{m}$ is the magnetic dipole moment and $\hat{n}$ is the unit vector in the direction of $\vec{x}$. To calculate the magnetic field of the whole magnet, we integrate over its volume the contributions from the infinitesimal dipoles, either of the scalar potential or of the field. In the first case, we take finally $\vec{B} = -\mu_0\nabla\Phi$. The decision of which way to go depends on the ease of calculation in each case. In particular, the configurations with azimuthal symmetry offer the use of interesting mathematical properties. The basic idea is to find the scalar potential on the symmetry axis (z axis in our case), which is relatively easy to calculate, and from this function the solution is built for off-axis points. For example, Jackson [10] used successive derivatives of the axial function to find the magnetic field due to a solenoid. In this work we use a property of the solutions of the Laplace equation. This property, which is often used in the case of the electrostatic potential, [5,9] states that if you have the solution on the symmetry axis expressed as a series:

$$\Phi_{\text{axis}}(z) = \sum_{\ell=0}^{\infty}\left(U_\ell z^\ell + \frac{V_\ell}{z^{\ell+1}}\right) \quad (2)$$

then the solution at any point in space (r,θ) is given by:

$$\Phi(r,\theta) = \sum_{\ell=0}^{\infty}\left(U_\ell r^\ell + \frac{V_\ell}{r^{\ell+1}}\right)P_\ell(\cos\theta)$$

where $P_\ell(\cos\theta)$ is the Legendre polynomial of order ℓ. Therefore, all we have to do is to calculate $\Phi_{\text{axis}}(z)$ and expand it in powers of z. Now, we illustrate this approach with the case of a spherical magnet.

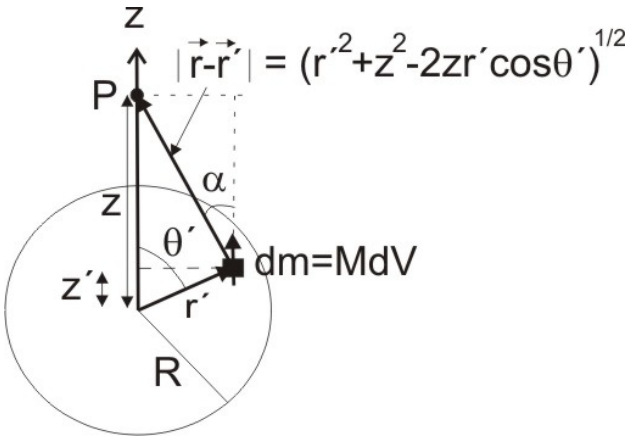

FIGURE 1. Scheme for calculating the field produced by a spherical magnet.

2.1. Sphere

According to Fig. 1, we write the contribution of each infinitesimal dipole as:

$$d\Phi_{\text{axis}}(z) = \frac{1}{4\pi}\frac{dm\cdot\cos\alpha}{|\vec{r}-\vec{r'}|^2} = \frac{1}{4\pi}\frac{MdV(z-z')}{(z^2+r'^2-2zr'\cos\theta')^{3/2}}$$

The total scalar potential on the z axis is then given by:

$$\Phi_{\text{axis}}(z) = \frac{M}{4\pi}\int_0^{2\pi}d\phi'\int_0^{\pi}\sin\theta' d\theta' \times\int_0^{R}\frac{r'^2(z-r'\cos\theta')}{(z^2+r'^2-2zr'\cos\theta')^{3/2}}dr' = \frac{M}{2}\int_0^{R}r'^2dr'\int_{-1}^{1}\frac{z-r'x}{(z^2+r'^2-2zr'x)^{3/2}}dx$$

By using *Mathematica*, we find the indefinite integral in x results

$$\frac{-r'+xz}{z^2(r'^2-2r'xz+z^2)^{1/2}}$$

Evaluating in the limits and simplifying, we obtain $2/z^2$, which does not depend on r'. Finally, performing the integration on this variable, we obtain

$$\Phi_{\text{axis}}(z) = \frac{MR^3}{3}\frac{1}{z^2} \quad (3)$$

The last expression is a particular case of Eq. (2), with coefficients $U_\ell = 0\ \forall\ell$ and $V_1 = MR^3/3$, $V_\ell = 0\ \forall\ell \neq 1$. Applying the property described above, we see that the potential at any point in space is given by:

$$\Phi(r,\theta) = \frac{MR^3}{3}\frac{1}{r^2}P_1(\cos\theta) = \frac{MR^3}{3}\frac{\cos\theta}{r^2} = \frac{1}{4\pi}\frac{m\cos\theta}{r^2}$$

where $m = 4\pi MR^3/3$ is the magnetic dipole moment of the sphere. This result is well known and is equivalent to that produced by a point dipole with moment m placed at the center of the sphere, as can be seen from Eq. (1). As mentioned above, the induction field is given by $\vec{B}(r,\theta) = -\mu_0\nabla\Phi(r,\theta)$. Next, we present the results of the magnetic field on the axis of symmetry of the other magnets, and compare them with measurements made in the laboratory.

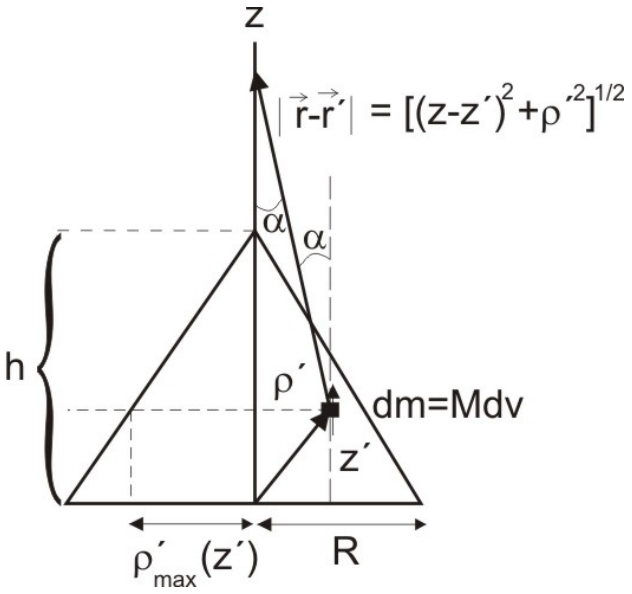

FIGURE 2. Scheme for calculating the field produced by a conical magnet.

2.2. Cone

According to Fig. 2, each infinitesimal dipole contributes to the potential on the z axis with:

$$d\Phi_{\text{axis}}(z) = \frac{1}{4\pi}\frac{dm\cos\alpha}{|\vec{r}-\vec{r'}|^2} = \frac{1}{4\pi}\frac{M\rho' d\rho' dz' d\phi'(z-z')}{[(z-z')^2+\rho'^2]^{3/2}}$$

Therefore, the potential on the axis is given by

$$\begin{aligned}\Phi_{\text{axis}}(z) &= \frac{M}{4\pi}\int_0^{2\pi} d\phi' \int_0^h (z-z')dz' \\ &\times \int_0^{\rho'_{\text{max}}(z')} \frac{\rho' d\rho'}{[(z-z')^2+\rho'^2]^{3/2}} \\ &= \frac{M}{2}\int_0^h (z-z')dz' \int_0^{R(1-\frac{z'}{h})} \frac{\rho' d\rho'}{[(z-z')^2+\rho'^2]^{3/2}} \\ &= \frac{Mh}{2} - \frac{M}{2}\int_0^h \frac{(z-z')dz'}{[(z-z')^2+R^2(1-\frac{z'}{h})^2]^{1/2}}\end{aligned}$$

The additive constant is irrelevant and can be suppressed. With the change of variable $x = z - z'$, we can write

$$\Phi_{\text{axis}}(z) = \frac{M}{2}\int_z^{z-h} \frac{xdx}{[Dx^2+Ex+F]^{1/2}}$$

where

$$D = 1+\frac{R^2}{h^2},\ E = \frac{2R^2}{h}\left(1-\frac{z}{h}\right),\ F = R^2\left(1-\frac{z}{h}\right)^2.$$

After integrating, evaluating in the limits and simplifying, we finally obtain:

$$\begin{aligned}\Phi_{\text{axis}}(z) &= \frac{Mh^2}{2(h^2+R^2)}\left[\pm(z-h)-\sqrt{R^2+z^2}\right] \\ &+ \frac{MhR^2(z-h)}{2(h^2+R^2)^{3/2}} \\ &\times \ln\frac{(h\pm\sqrt{h^2+R^2})(z-h)}{R^2+hz+\sqrt{h^2+R^2}\sqrt{R^2+z^2}}\end{aligned} \tag{4}$$

Then, the induction field has the following dependence on the z axis:

$$\begin{aligned}B(z) = \frac{\mu_0 Mh}{2}\Bigg[&\frac{1}{h^2+R^2}\left(\frac{zh-R^2}{\sqrt{R^2+z^2}}\mp h\right) \\ &- \frac{R^2}{(h^2+R^2)^{3/2}}\ln\frac{(h\pm\sqrt{h^2+R^2})(z-h)}{R^2+hz+\sqrt{h^2+R^2}\sqrt{R^2+z^2}}\Bigg]\end{aligned} \tag{5}$$

The double sign in the Eqs. (4) and (5) apply to the values of z above the apex of the magnet ($z > h$, upper sign) or below the base ($z < h$, lower sign). Interestingly, the model predicts that field diverges at the apex of the magnet. This feature is the basis of the design of electromagnets with truncated conical poles, which produce high magnetic fields. The variation of this field along the z axis was calculated by Kroon [11].

2.3. Cylinder

As shown in Fig. 3 (b), the potential on the z axis due to each infinitesimal dipole is given by:

$$d\Phi_{\text{axis}} = \frac{1}{4\pi}dm\frac{\cos\theta'}{|\vec{r}-\vec{r'}|^2} = \frac{1}{4\pi}MdV\frac{z-z'}{|\vec{r}-\vec{r'}|^3} = \frac{M}{4\pi}\frac{z-z'}{[(z-z')^2+\rho'^2]^{3/2}}\rho' d\rho' dz' d\phi'$$

Therefore, the total scalar potential on the axis is given by:

$$\Phi_{\text{axiz}}(z) = \frac{M}{4\pi}\int_{\text{cylinder}} \frac{z-z'}{[(z-z')^2+\rho'^2]^{3/2}}\rho' d\rho' dz' d\phi' = \frac{M}{2}\int_0^L (z-z')dz' \int_0^R \frac{\rho' d\rho'}{[(z-z')^2+\rho'^2]^{3/2}}$$

$$= \frac{M}{2}\int_0^L (z-z')dz'\left(-\frac{1}{\sqrt{(z-z')^2+\rho'^2}}\Bigg|_{\rho'=0}^{\rho'=R}\right) = \frac{M}{2}\sqrt{(z-z')^2+\rho'^2}\Bigg|_{z'=0}^{z'=L}\Bigg|_{\rho'=0}^{\rho'=R}$$

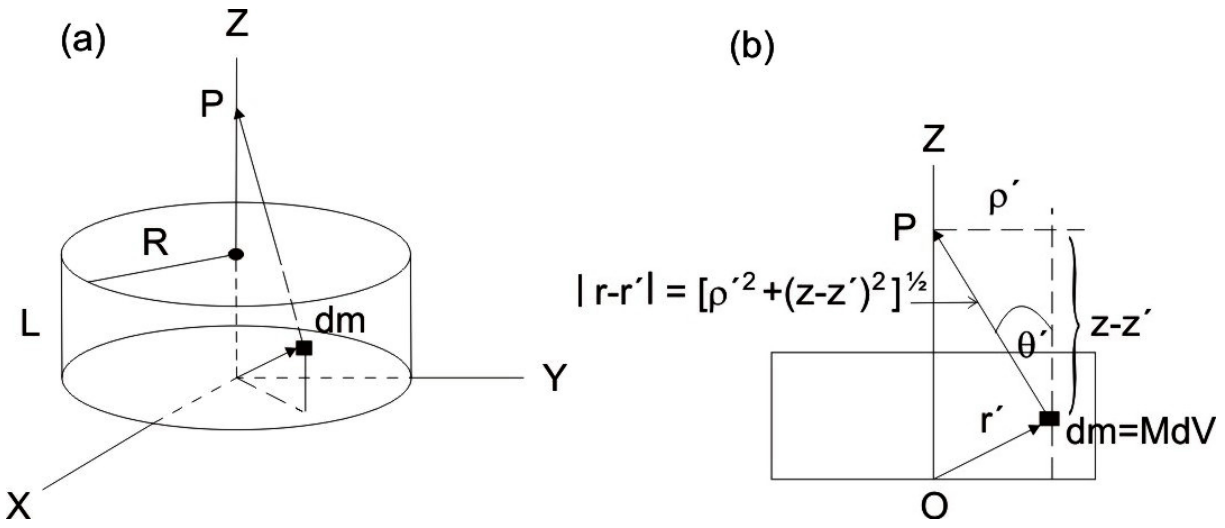

FIGURE 3. (a) Schematic of a cylindrical magnet. (b) Scheme for calculating the field produced by the magnet.

Ignoring additive constants, the resulting scalar potential is:

$$\Phi_{\text{axiz}}(z) = \frac{M}{2}\left(\sqrt{(z-L)^2+R^2} - \sqrt{z^2+R^2}\right) \quad (6)$$

Finally, the field on the z axis is given by:

$$B(z) = \frac{\mu_0 M}{2}\left(\frac{z}{\sqrt{z^2+R^2}} - \frac{z-L}{\sqrt{(z-L)^2+R^2}}\right) \quad (7)$$

2.4. Ring

The field produced by a ring magnet of outer radius R_1 and inner radius R_2 is obtained by the principle of superposition, adding the fields produced by a cylindrical magnet with magnetization $+M\hat{z}$ and radius R_1, and another cylinder with magnetization $-M\hat{z}$ and radius R_2. In terms of Fig. 4, the scalar potential and the field on the axis are given by:

$$\Phi_{\text{axiz}}(z) = \frac{M}{2}\left[\left(\sqrt{(z-L)^2+R_1^2} - \sqrt{z^2+R_1^2}\right) - \left(\sqrt{(z-L)^2+R_2^2} - \sqrt{z^2+R_2^2})\right)\right] \quad (8)$$

$$B(z) = \frac{\mu_0 M}{2}\left[\left(\frac{z}{\sqrt{z^2+R_1^2}} - \frac{z-L}{\sqrt{(z-L)^2+R_1^2}}\right) - \left(\frac{z}{\sqrt{z^2+R_2^2}} - \frac{z-L}{\sqrt{(z-L)^2+R_2^2}}\right)\right] \quad (9)$$

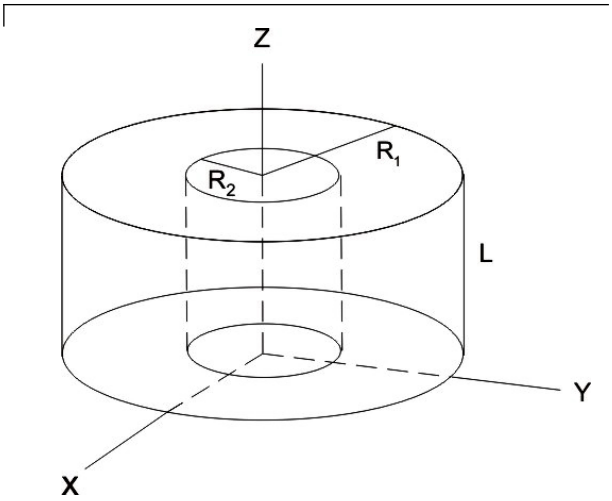

FIGURE 4. Schematic of a ring magnet.

2.5. Rectangular prism

Even though we cannot apply the theorem on magnets with azimuthal symmetry in this case, we calculated the field on the z axis (defined in the direction of magnetization of the magnet, *i.e.* $\vec{M} = M\hat{k}$). According to Fig. 5, we have:

$$d\Phi_{\text{axis}}(z) = \frac{1}{4\pi}\frac{dm\cos\theta'}{|\vec{r}-\vec{r'}|^2} = \frac{1}{4\pi}MdV\frac{z-z'}{|\vec{r}-\vec{r'}|^3} = \frac{M}{4\pi}\frac{z-z'}{[x'^2+y'^2+(z-z')^2]^{3/2}}dx'dy'dz'$$

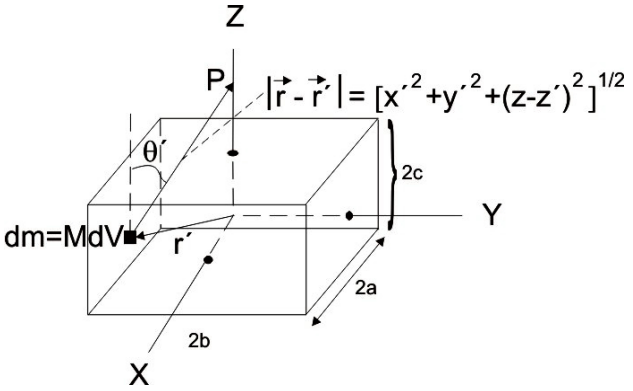

FIGURE 5. Scheme for calculating the field of a prism-shaped magnet.

Therefore,the potential on the z axis is given by:

$$\Phi_{\text{axis}}(z) = \frac{M}{4\pi}\int_{-c}^{c} dz'(z-z')\int_{-b}^{b} dy' \times \int_{-a}^{a} \frac{dx'}{[x'^2+y'^2+(z-z')^2]^{3/2}}$$

Integration on x' gives

$$\frac{x'}{[y'^2+(z-z')^2]\sqrt{x'^2+y'^2+(z-z')^2}}\Bigg|_{-a}^{a} = \frac{2a}{[y'^2+(z-z')^2]\sqrt{a^2+y'^2+(z-z')^2}}$$

Integration of this result on y' gives

$$\frac{2}{z-z'}\arctan\frac{ay'}{(z-z')\sqrt{a^2+y'^2+(z-z')^2}}\Bigg|_{-b}^{b} = \frac{4}{z-z'}\arctan\frac{ab}{(z-z')\sqrt{a^2+b^2+(z-z')^2}}$$

Then, we obtain:

$$\Phi_{\text{axis}}(z) = \frac{M}{\pi}\int_{-c}^{c}\arctan\frac{ab}{(z-z')\sqrt{a^2+b^2+(z-z')^2}}dz'$$

Mathematica gives (except additive constants omitted here):

$$\Phi_{\text{axis}}(z) = \frac{M}{\pi}\left[(z+c)\arctan\frac{ab}{(z+c)\sqrt{a^2+b^2+(z+c)^2}} - (z-c)\arctan\frac{ab}{(z-c)\sqrt{a^2+b^2+(z-c)^2}}\right] \quad (10)$$

Finally, the field on the axis is given by:

$$B(z) = \frac{\mu_0 M}{\pi}\left[\arctan\frac{ab}{(z-c)\sqrt{a^2+b^2+(z-c)^2}} - \arctan\frac{ab}{(z+c)\sqrt{a^2+b^2+(z+c)^2}}\right] \quad (11)$$

For completeness we reproduce here the results of Yang *et al*, [12] who calculated the magnetic field at any point in space. Adapting their results to the case of a magnetization directed along the z axis, we get:

$$B_x(x,y,z) = \frac{\mu_0 M}{4\pi}\ln\frac{F_2(-x,y,-z)F_2(x,y,z)}{F_2(x,y,-z)F_2(-x,y,z)}$$

$$B_y(x,y,z) = \frac{\mu_0 M}{4\pi}\ln\frac{F_2(-y,x,-z)F_2(y,x,z)}{F_2(y,x,-z)F_2(-y,x,z)}$$

$$B_z(x,y,z) = -\frac{\mu_0 M}{4\pi}\Big[F_1(-x,y,z)+F_1(-x,y,-z) + F_1(-x,-y,z)+F_1(-x,-y,-z) + F_1(x,y,z)+F_1(x,y,-z) + F_1(x,-y,z)+F_1(x,-y,-z)\Big]$$

The functions F_1 and F_2 are defined as:

$$F_1(x,y,z) = \arctan\frac{(x+a)(y+b)}{(z+c)\sqrt{(x+a)^2+(y+b)^2+(z+c)^2}}$$

$$F_2(x,y,z) = \frac{\sqrt{(x+a)^2+(y-b)^2+(z+c)^2}+b-y}{\sqrt{(x+a)^2+(y+b)^2+(z+c)^2}-b-y}$$

We can easily check that the x and y field components vanish on the z axis, while the z component is reduced to the expression given in Eq. (11).

3. Results of magnetic fields on the z axis and comparison with experiments

Now we compare the theoretical calculations of magnetic fields on the symmetry axis with measurements made in the laboratory. First, from Eq. (3) we obtain the field for the sphere:

$$B(z) = \frac{2\mu_0 M R^3}{3z^3} \quad (12)$$

We measured the magnetic field using a gaussmeter with an estimated accuracy of $\pm 5\%$. From a linear fitting of this field vs. $1/z^3$, we obtained a magnetization value $\mu_0 M = (0.933 \pm 0.044)$ T, which lies in the range expected in these magnets. For example, A. Walther *et. al*. [13] reported a value of 1.25 T for thin films of $Nd_2Fe_{14}B$; in the case of single crystals it has been reported [14,15] a value of 1.6 T at room temperature. The magnetization of the other

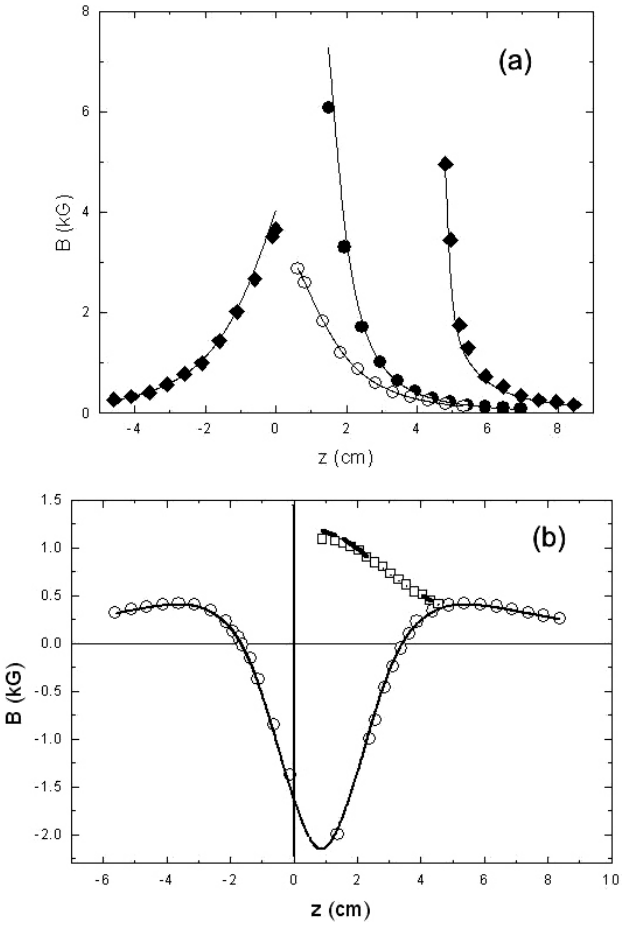

FIGURE 6. (a). Magnetic field measurements as a function of axial distance for a sphere (◯), a cone (♦) and a prism (•). Solid lines correspond to theoretical calculations (Eqs. 12, 5 and 11, respectively) using the values of magnetization shown in Table I. (b). Magnetic field measurements as a function of axial distance for the case of a cylinder (□) and a ring (◯). Solid lines correspond to theoretical calculations (Eqs. 7 and 9, respectively) using the values of magnetization shown in Table I.

TABLE I. Volumetric magnetization and dimensions of all magnets used in this work.

Magnet	$\mu_0 M(T)$	Dimensions (cm)
Sphere	0.933 ± 0.044	R=1.5
Cone	1.103 ± 0.027	$R = 2.46, h = 4.80$
Cylinder	0.830 ± 0.031	$R = 3.81, L = 1.27$
Ring	1.086 ± 0.028	$R_1 = 5.35, R_2 = 2.25, L = 1.75$
Prism	0.870 ± 0.070	$2a = 5.0, 2b = 2.5, 2c = 1.25$

magnets was obtained accordingly by scaling each theoretical function (Eqs. (5), (7), (9) and (11)) to its corresponding measured field. Table I shows the magnetization of all magnets and their geometric dimensions.

Figure 6 shows the measured and calculated field as a function of axial distance for (a) sphere, cone and prism, and (b) cylinder and ring.

The ring magnet offers several particular aspects. The first is the possibility of measuring the field in a continuous manner through the magnet gap, resulting in a larger number of experimental points. The second is the existence of two points placed symmetrically on the shaft (at $z = -1.80$ cm and $z = 3.55$ cm) where the field becomes zero. To verify this, we placed a very small magnet (1 mm thick and 1 mm radius) in the vicinity of those positions and slid it along the z axis with care. It was very interesting to see the small magnet turning around due to the change of sign of the field.

In general terms, we conclude that the agreement shown in Fig. 6 between theory and experiment is quite good. We can say that the method of calculation describes fairly well the field on the axis of permanent magnets with different geometries.

Next, we focus on the calculation of the field outside the symmetry axis for the case of the cylindrical magnet. This will illustrate the use of the series expansion given in Eq. (2).

4. Field of a cylindrical magnet for points outside the axis of symmetry

4.1. Analytical calculation

We tried to calculate $\Phi(\rho, z)$ using *Mathematica*, but did not succeed. Then, we intented to perform the intergration with *Maple* but we failed too. Our next attempt was to calculate the vector potential, which has the form $\vec{A}(\rho, z) = A(\rho, z)\hat{\phi}$. Explicitly, we have:

$$A(\rho, z) = \frac{\mu_0 RM}{4\pi} \int_0^L dz' \times \int_0^{2\pi} \frac{\cos\phi' d\phi'}{\sqrt{\rho^2 + R^2 + (z - z')^2 - 2R\rho\cos\phi'}}$$

In the first place, we calculated the component B_ρ along the radius of the cylinder:

$$B_\rho(\rho, z) = -\frac{\partial A}{\partial z} = \frac{\mu_0 RM}{4\pi} \times \int_0^{2\pi} \frac{\cos\phi' d\phi'}{\sqrt{\rho^2 + R^2 + (z - z')^2 - 2R\rho\cos\phi'}} \Bigg|_{z'=0}^{z'=L}$$

By using *Maple*, we obtained:

$$B_\rho(\rho, z) = \frac{\mu_0 M}{2\pi}\sqrt{\frac{R}{\rho}}\left[F\left(\alpha(z'), \frac{1}{\alpha(z')}\right) - 2E\left(\alpha(z'), \frac{1}{\alpha(z')}\right)\right]\Bigg|_{z'=0}^{z'=L}$$

where

$$\alpha(z') = 2\sqrt{\frac{R\rho}{(\rho + R)^2 + (z - z')^2}}$$

and $F(x,y)$ and $E(x,y)$ are the Incomplete Elliptical Integrals of first and second class respectively.

To calculate the vertical component of the field, we need to take

$$B_z(\rho,z) = \frac{1}{\rho}\frac{\partial(A\rho)}{\partial\rho}$$

Unfortunately, none of the programs that we tried (*Mathematica* and *Maple*) were able to provide an analytical result in this case. As we can see, the magnetic induction field outside the cylinder axis is difficult to obtain. In several previous interesting works published in educational journals, the field of cylindrical magnets or solenoids has been calculated. For example, Labinac *et al* [16] calculated the field for a thin solenoid and a thick coil using a series expansion of Gauss hypergeometric functions. Derby and Olbert [17] calculated the field from a solenoid to study the speed of fall of permanent cylindrical magnets inside a copper tube. Lerner [18] analyzed the role of the permeable core of a finite solenoid, by comparing its field with that produced by an infinite solenoid. In each case, the calculation involved elliptic integrals, whose evaluation is difficult. This is where the expansion of $\Phi_{\text{axis}}(z)$ proposed in the present work will exhibit its usefulness.

4.2. Force between two cylindrical magnets

As we just showed, it is very difficult to obtain closed expressions of the field for a cylindrical magnet. To illustrate the method of approximation in power series, we decided to calculate the force between two cylindrical magnets with uniform magnetization, and compare our results with experimental measurements. Before that, we want to mention that similar calculations have been reported previously. The force between two cubic magnets was calculated analytically by Akoun *et. al* [19]. Also, recently it has been possible to calculate the torque between these magnets [20].

To realize our study, we placed the two magnets coaxially as shown in Fig. 7. The vertical force was measured with a Pasco Scientific CI-6537 sensor mounted onto a homemade universal base. The upper magnet was attached to the sensor and the lower one was attached to a mobile stage which could be displaced vertically with a screw. Each 360° turn of the screw produced a displacement of 1.49 mm. This way, the distance between the magnets (a) could be varied with a high precision. The sensor has an accuracy of ± 0.03 N.

The force exerted by magnet 1 on magnet 2 is given by

$$\vec{F} = \int\limits_{\text{magnet}-2} \nabla(d\vec{\mu}\cdot\vec{B})$$

Here, $\vec{B}$ is the the field produced by the lower magnet. More specifically, the vertical force is

$$F = \int_{\text{magnet}-2} M_2 \frac{\partial B_z}{\partial z} dV \qquad (13)$$

The first step of the calculation is to expand the function given by Eq. (6) in powers of z. The terms to expand can be written in the form:

$$\sqrt{1+x^2} = 1 + \frac{1}{2}x^2 - \frac{1}{8}x^4 + \frac{1}{16}x^6 - \frac{5}{128}x^8 + \ldots$$

This expansion is valid for $|x| < 1$. For this reason, if $R > L$, three regions are defined: close ($L < z < R$), intermediate ($R < z < L + R$) and far ($z > L + R$). If $L > R$ no close region exists; only the intermediate ($L < z < L + R$) and far ($z > L + R$) regions remain. Since $R_1 = 1.27$ cm > 0.95 cm $= L_1$, we need to consider the three regions .

The infinite series can be truncated by taking a finite number of terms, up to a maximum power of z (ℓ_{max}). The approximation to the exact potential improves as more terms are included, but the calculation of the force becomes increasingly

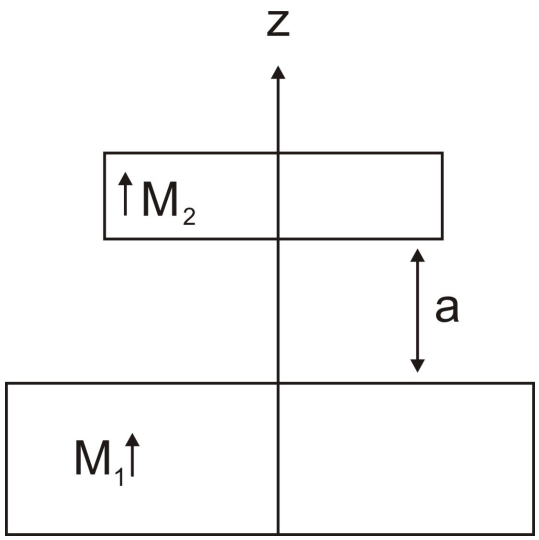

FIGURE 7. Arrangement of two coaxial cylindrical magnets, whose repulsive force was measured and calculated. The experimental parameters are: $\mu_0 M_1 = 0.89$ T, $R_1 = 1.27$ cm, $L_1 = 0.95$ cm, $\mu_0 M_2 = 0.92$ T, $R_2 = 0.635$ cm, $L_2 = 0.485$ cm

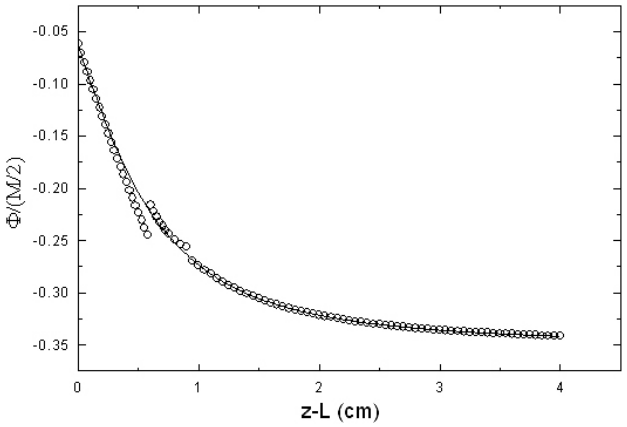

FIGURE 8. Magnetic scalar potential on the axis of the magnet 1, normalized to the value $M/2$, for points outside the magnet (*i. e.* for $z > L$). We show the finite series expansion, Eq. (2) with coefficients given in the appendix (◯), and the exact Eq. (6) (solid line).

elaborate. The choice of $\ell_{\max}$ depends on these two factors. The expansion coefficients for each zone are listed in the appendix. The coefficients were taken up to the greatest value the computer could handle ($\ell_{\max}$ = 10, 9 or 8).

Figure 8 shows the plots of the exact potential due to the magnet 1 on its axis, and the approximation of the finite series. As it can be seen, the approximation is quite good except near the borders between neighbor zones ($z - L_1$ = 0.58 and 0.93 cm), where convergence of the series is slower. As mentioned, one uses a certain number of terms to give a good balance between accuracy and computation time. In Ref. 7, the author used up to 20 terms in the series he proposed, getting an excellent agreement with the exact calculation; however, he found discrepancies of the order of 100% in certain regions. In our example, the maximum difference observed with respect to the exact value on the axis was about 15%. We just want to bring in the idea that in any finite series approximation, there will be regions of very slow convergence, in which there will be significant deviations from the exact function.

Now, it is interesting to take a close view at the explicit expression in the far region. The series expansion is:

$$\Phi_{\text{axis}}(z) = \frac{M}{2}\sum_{k=1}^{\infty}\sum_{i=1}^{\infty} L^i R^{2k} \binom{1/2}{k}\binom{2k-2+i}{2k-2}\frac{1}{z^{2k-1+i}}$$

Therefore, the scalar potential at any point of this region is given by:

$$\Phi(r,\theta) = \frac{M}{2}\left(\frac{LR^2}{2}\frac{\cos\theta}{r^2} + \frac{L^2R^2}{4}\frac{3\cos^2\theta - 1}{r^3} + \frac{4L^3R^2 - 3LR^4}{16}\frac{5\cos^3\theta - 3\cos\theta}{r^4} + \ldots\right) \quad (14)$$

This expression resembles the multipole expansion of the electrostatic potential $\Phi_{\rho_e}(\vec{x})$ outside the region containing all source charges [9]:

$$\Phi_{\rho_e}(\vec{x}) = \frac{1}{4\pi\epsilon_0}\left(\frac{q}{r} + \frac{\vec{p}\cdot\hat{x}}{r^2} + \frac{1}{2}\sum_{i,j} Q_{ij}\frac{\hat{x_i}\hat{x_j}}{r^3} + \cdots\right)$$

where

$$q = \int \rho_e d^3x$$

is the total charge,

$$\vec{p} = \int \vec{x}\rho_e d^3x$$

is the dipole moment of the charge distribution,

$$Q_{ij} = \int (3x_i x_j - r^2\delta_{ij})\rho_e d^3x$$

is the traceless quadrupole moment tensor, ρ_e is the charge density, ϵ_0 is the vacuum permitivity and $r = \mid \vec{x} \mid$. Griffiths [21] presents a nice graphic discussion of the latter expansion. The first term is the monopole contribution to the potential and goes like $1/r$, the second term corresponds to the dipolar distribution and goes like $1/r^2$, the third term is the quadrupole one and goes like $1/r^3$, the octupole term goes like $1/r^4$, and so on. Therefore, it is possible to identify Eq. (14) as the multipole expansion of the magnetic scalar potential produced by the permanent magnet. As expected, the monople term vanishes because of the nonexistence of magnetic monopoles. The leading term in this equation is

$$\frac{MLR^2}{4}\frac{\cos\theta}{r^2} = \frac{1}{4\pi}\frac{m\cos\theta}{r^2},$$

i.e., the dipole contribution. In all the geometries studied here, we expanded $\Phi_{\text{axis}}(z)$ in a power series of $1/z$ around zero. We found in every case that the dipole contribution given by Eq. (1) was the leading term, which makes a lot of sense since at large distances the magnet "looks" like a point dipole. The similiarity between the electrostatic multipole expansion and the present one is not casual: it is easy to demonstrate [22] that the scalar potential due to a uniformly magnetized body of arbitrary form may be written in the form $\Phi = -\vec{M}\cdot\nabla(\epsilon_0\psi)$, where ψ is the electrostatic potential due to a uniformly charged body (with $\rho_e = 1$) of the same form and dimensions. Indeed, the dipole term of the magnet expansion (14) can be obtained by applying the latest formula to the monople term of the expansion of $\Phi_{\rho_e}(\vec{x})$, with $\rho_e = 1$. The second term of Eq. (14) can be obtained from the second term of the electrostatic series, an so on. Therefore, there exists a tight connection between electrostatic and magnetostatic potentials due to uniform sources, and the present calculation is a nice and educational manifestation of this characteristic.

Next, we calculated the vertical component of the magnetic induction field:

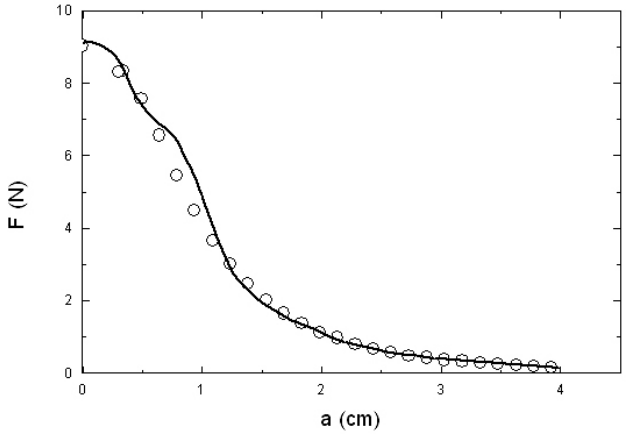

FIGURE 9. Force between the two cylindrical magnets as a function of their separation distance a. We show the measured values (◯) and the calculated ones using the method described in the text (solid line).

$$B_z(r,\theta) = -\mu_0 \frac{\partial \Phi(r,\theta)}{\partial z}$$

and changed from spherical (r,θ) to cylindrical coordinates (ρ, z) before performing the integral of Eq. (13) to obtain the vertical force between the two magnets. The expressions are too large to be reproduced here, therefore we preferred to present the results in a plot. The *Mathematica* file containing the full expression of the force in the far region (the simplest case) can be downloaded freely at[i]

Figure 9 shows the force F as a function of a. We can see that the theoretical calculation describes fairly well the experimental behavior. Comparing Figs. 8 and 9, we see that the largest differences between model and experiment occur near the boundaries between zones of the potential expansion. Apart from these discrepancies, we can say that our method works adequately. This methodology was used to calculate the force between a cylinder magnet and a superconductor in the Meissner state [23]. The interaction between a ring magnet and any other magnet can be studied using the principle of superposition and a similar approach to the one followed in this section. The task of calculating with this method the field outside the axis of symmetry for the cone magnet is left to smart challenge hunters.

5. Conclusions

An alternative method to calculate the magnetic field at any point in space produced by a permanent magnet with azimuthal symmetry is presented. The method is based on a power series expansion of the magnetic scalar potential value on the axis of symmetry. The resulting series can be identified as the multipole expansion of the potential. This approach allowed us to obtain the force between cylindrical magnets without using the hard-to-manage exact solutions. The magnetic fields on the axis of a sphere, rectangular prism, cone, cylinder and ring were calculated. The calculations showed good agreement with the experiments.

6. Appendix

Coefficients of the expansion of the scalar magnetic potential on the symmetry axis for a cylindrical magnet.

$$\Phi_{\text{axis}}(z) = \frac{M}{2} \sum_{\ell=0}^{\infty} \left(U_\ell^+ z^\ell + \frac{V_\ell^+}{z^{\ell+1}} \right)$$

6.1. Close region

$$V_\ell^+ = 0 \quad \forall \ell$$

ℓ	U_ℓ^+
0	$\frac{L^2}{2R} - \frac{L^4}{8R^3} + \frac{L^6}{16R^5} - \frac{5L^8}{128R^7} + \frac{7L^{10}}{256R^9}$
1	$-\frac{L}{R} + \frac{L^3}{2R^3} - \frac{3L^5}{8R^5} + \frac{5L^7}{16R^7} - \frac{35L^9}{128R^9}$
2	$-\frac{3L^2}{4R^3} + \frac{15L^4}{16R^5} - \frac{35L^6}{32R^7} + \frac{315L^8}{256R^9}$
3	$\frac{L}{2R^3} - \frac{5L^3}{4R^5} + \frac{35L^5}{16R^7} - \frac{105L^7}{32R^9}$
4	$\frac{15L^2}{16R^5} - \frac{175L^4}{64R^7} + \frac{735L^6}{128R^9}$
5	$-\frac{3L}{8R^5} + \frac{35L^3}{16R^7} - \frac{441L^5}{16R^9}$
6	$-\frac{35L^2}{32R^7} + \frac{735L^4}{128R^9}$
7	$\frac{5L}{16R^7} - \frac{105L^3}{32R^9}$
8	$\frac{315L^2}{256R^9}$
9	$-\frac{35L}{128R^9}$

6.2. Intermediate region

ℓ	U_ℓ^+	V_ℓ^+
0	$R + \frac{L^2}{2R} - \frac{L^4}{8R^3} + \frac{L^6}{16R^5} - \frac{5L^8}{128R^7} + \frac{7L^{10}}{256R^9}$	$-\frac{R^2}{2}$
1	$1 - \frac{L}{R} + \frac{L^3}{2R^3} - \frac{3L^5}{8R^5} + \frac{5L^7}{16R^7} - \frac{35L^9}{128R^9}$	0
2	$\frac{1}{2R} - \frac{3L^2}{4R^3} + \frac{15L^4}{16R^5} - \frac{35L^6}{32R^7} + \frac{315L^8}{256R^9}$	$\frac{R^4}{8}$
3	$\frac{L}{2R^3} - \frac{5L^3}{4R^5} + \frac{35L^5}{16R^7} - \frac{105L^7}{32R^9}$	0
4	$-\frac{1}{8R^3} + \frac{15L^2}{16R^5} - \frac{175L^4}{64R^7} + \frac{735L^6}{128R^9}$	$-\frac{R^6}{16}$
5	$-\frac{3L}{8R^5} + \frac{35L^3}{16R^7} - \frac{441L^5}{64R^9}$	0
6	$\frac{1}{16R^5} - \frac{35L^2}{32R^7} + \frac{735L^4}{128R^9}$	$\frac{5R^8}{128}$
7	$\frac{5L}{16R^7} - \frac{105L^3}{32R^9}$	0
8	$-\frac{5}{128R^7} + \frac{315L^2}{256R^9}$	$-\frac{7R^{10}}{256}$
9	$-\frac{35L}{128R^9}$	0
10	$\frac{7}{256R^9}$	$\frac{21R^{12}}{1024}$

6.3. Far region

$$U_\ell^+ = 0 \qquad \forall \ell$$

ℓ	V_ℓ^+
0	0
1	$\frac{LR^2}{2}$
2	$\frac{L^2R^2}{2}$
3	$\frac{4L^3R^2-3LR^4}{8}$
4	$\frac{2L^4R^2-3L^2R^4}{4}$
5	$\frac{8L^5R^2-20L^3R^4+5LR^6}{16}$
6	$\frac{8L^6R^2-30L^4R^4+15L^2R^6}{16}$
7	$\frac{64L^7R^2-336L^5R^4+280L^3R^6-35LR^8}{128}$
8	$\frac{16L^8R^2-112L^6R^4+140L^4R^6-35L^2R^8}{32}$

Acknowledgments

Authors thank M.C. Fidel Gamboa and Ing. Osvaldo Gómez for their technical assistance.

i. http://www.mda.cinvestav.mx/magnetic_forces/force_in_the_far_region.nb.

1. D. Castelvecchi, *Sci. Amer.* **306** (2012) 37-41.
2. L. Holysz, A. Szczes, and E. Chibowski, *J. Colloid Interface Sci.* **316** (2007) 996-1002.
3. X. F. Pang and B. Deng, *Physics Mechanics Astron.* **51** (2008) 1621-1632.
4. R. Cai, H. Yang, J. He, and W. Zhu, *J. Mol. Struct.* **938** (2009) 15-19.
5. Jr. Stanley Humphries, *Finite-element methods for electromagnetics* (2010). Electronic document available at http://www.fieldp.com/femethods.html
6. P. Pao-la-or, A. Isaramongkolrak, and T. Kulworawanichpong, *Engineering Lett.* **18** (2010). Online document available at http://www.engineeringletters.com/issues_v18/issue_1/EL_18_1_01.pdf
7. R. Ravaud, G. Lemarquand, V. Lemarquand and C. Depollier, *IEEE Trans. Magn.* **44** (2008) 1982-1989.
8. R. Ravaud, G. Lemarquand, V. Lemarquand and C. Depollier, *PIER B* **11** (2009) 281-297.
9. J. D. Jackson, *Classical Electrodynamics*, third edition, (Wiley, 1998).
10. R. H. Jackson, *IEEE Trans. Electr. Dev.* **46** (1999) 1050-1062.
11. D. J. Kroon, *Electromagnets* (Boston Technical Publishers Inc., Philips Technical Library, 1968). pp. 15-19.
12. Z. J. Yang, T. Johansen, H. Bratsberg, G. Helgesen and A. T. Skjeltorp, *Supercond. Sci. Technol.* **3** (1990) 591.
13. A. Walther, C. Marcoux, B. Desloges, R. Grechishkin, D. Givord, N. M. Dempsey, *J. Magn. Magn. Mater.* **321** (2009) 590-594.
14. M. Sagawa, S. Fujimura, H. Yamamoto, Y. Matsuura, and S. Hirosawa, *J. Appl. Phys.* **57** (1985) 4094-4098.
15. J. F. Herbst, *Rev. Mod. Phys.* **63** (1991) 819-898.
16. V. Labinac, N. Erceg, and D. Kotnik-Karuza, *Am. J. Phys.* **74** (2006) 621-627.
17. N. Derby and S. Olbert, *Am. J. Phys.* **78** (2010) 229-235.
18. L. Lerner, *Am. J. Phys.* **79** (2011) 1030-1035.
19. G. Akoun and J.-P. Yonnet, *IEEE Trans. Magn.* **20** (1984) 1962-1964.
20. H. Allag and J.-P. Yonnet, *IEEE Trans. Magn.* **45** (2009) 3969-3972.
21. D. J. Griffiths, *Introduction to Electrodynamics* third edition, (Prentice Hall 1999).
22. V. V. Batygin and I. N. Topygin, *Problems in Electrodynamics* (Academic Press, London 1964), see problem 287.
23. E. Várguez-Villanueva, V. Rodríguez-Zermeño, and V. Sosa, *Rev. Mex. Fís.* **54** (2008) 293-298.